Research Article Open Access

Amin Amini* and Hamidreza Ramazi

CRSP, numerical results for an electrical resistivity array to detect underground cavities

DOI 10.1515/geo-2017-0002
Received Oct 27, 2015; accepted Mar 12, 2016

Abstract: This paper is devoted to the application of the Combined Resistivity Sounding and Profiling electrode configuration (CRSP) to detect underground cavities. Electrical resistivity surveying is among the most favorite geophysical methods due to its nondestructive and economical properties in a wide range of geosciences. Several types of the electrode arrays are applied to detect different certain objectives. In one hand, the electrode array plays an important role in determination of output resolution and depth of investigations in all resistivity surveys. On the other hand, they have their own merits and demerits in terms of depth of investigations, signal strength, and sensitivity to resistivity variations. In this article several synthetic models, simulating different conditions of cavity occurrence, were used to examine the responses of some conventional electrode arrays and also CRSP array. The results showed that CRSP electrode configuration can detect the desired objectives with a higher resolution rather than some other types of arrays. Also a field case study was discussed in which electrical resistivity approach was conducted in Abshenasan expressway (Tehran, Iran) U-turn bridge site for detecting potential cavities and/or filling loose materials. The results led to detect an aqueduct tunnel passing beneath the study area.

Keywords: electrical resistivity imaging; CRSP array; cavity detection; Iran

1 Introduction

Electrical resistivity approach is one of the most widely used geophysical surveying methods. It could be applied in a wide variety of fields such as ground water and underground mineral explorations, Geotechnical and environmental investigations and archeological studies [1–5] and [6]. The purpose of electrical resistivity surveys is to determine underground resistivity contrasts by making measurements on the ground surface, which result in electrical anomalies of subsurface materials [7]. Electrical resistivity imaging has been developed to create accurate 2-D and 3-D computational resistivity models of subsurface cross-sections [9**?**], and [10]. In all resistivity surveys electrode configuration plays an important role in determination of output resolution and depth of investigation. Different electrode arrays have been introduced to be used in resistivity and/or IP surveys since 1920s, such as Schlumberger, Wenner, and dipole – dipole, each has its own merits and demerits. In this way some papers have devoted to numerical comparison of resolution and/or sensitivity between two or more electrode arrays over certain objectives [11–13], and [14].

Natural and man-made underground voids are of the most important objectives to be investigated for many engineering fields such as civil engineering projects, water resource engineering and archeology [15–18], and [19]. The problem is to detect the desired objective with an acceptable precision and a reasonable cost. Different prospecting techniques have been employed to detect underground voids. In this way, the electrical resistivity approach has been frequently used [20–22], and [23]. Underground voids such as caves, cellars, aqueduct tunnels, etc. can be empty or filled; they are not in the same geometry and are not occurred at a certain depth. Here the main problem is that none of conventional electrode arrays are able to be effective in all conditions. For instance, in one hand data acquired using a Wenner array are less contaminated by noise than the other electrode arrays; while the anomaly effects are relatively poor in the corresponding electrical resistivity images. On the other hand, despite of giving high resolution images, data arisen by dipole - dipole are susceptible to noise effects in deep direction [13]. The goal of this paper is to introduce combined resistivity sounding and profiling (CRSP) array as a suitable electrode array to detect cavities with various shapes in different depths of occurance. In this way, CRSP performance is examined in

***Corresponding Author: Amin Amini:** Amirkabir University of Technology, 424 Hafez Avenue, Tehran, Iran; Email: a.amini@aut.ac.ir; Tel.: +982164542926
Hamidreza Ramazi: Amirkabir University of Technology, 424 Hafez Avenue, Tehran, Iran

term of 1D sensitivity function; then, responses of different types of arrays applied to synthetic models are compared to corresponding results due to CRSP array. Also a field case study is discussed in which CRSP array was applied for engineering investigation of a bridge site in Tehran, Iran.

2 CRSP configuration

CRSP was introduced by [24] and is defined as follows: three vertical electrical soundings are surveyed simultaneously by a set of measurement current electrodes that are normally used for one vertical electrical sounding (VES). In this array the distance of each measuring station is equal to the spacing of the potential electrodes (Figure 1). As shown in the figure, CRSP is similar to the Schlumberger and Wenner-Schlumberger arrays in central measurements; however, the potential electrode spacing can be decreased for shorter current electrode distances and hence increased horizontal resolution. The potential electrode spacing depends on the survey's objectives, including its depth of investigation. We define 'n' as:

$$n = \frac{AB - P_c}{2P_c}$$

Where
AB is the current electrode spacing and P_c is the appropriate potential electrode spacing (P2P3 distance) which is equal to P_L and P_R. The first current electrode spacing in CRSP measurements starts at n=2 which is equal to five times the appropriate potential electrode spacing (including the measuring station interval). For example, if the measuring stations interval is 5 m (P1P2=P2P3=P3P4=5 m), the first current electrode spacing (AB) for CRSP measurements will be 25 m (AB=25 m). AB is increased for the other measurements as the following:

$$AB = P_c(2n + 1)$$

For n=1 the current electrode distance is equal to three times the potential electrode spacing (for example AB=15 m); in this case and also for other near surface measurements (AB<15 m), each the sounding points is surveyed individually as the Schlumberger array. The data obtained by this array could be processed and interpreted as sounding curves and/or into pseudo-sections. The CRSP array provides an enhanced lateral and in depth coverage, due to the acquisition of more data in a section (Figure 1). In practice, CRSP has been successfully applied to different mineral exploration and engineering site investigations [18, 25, 26], and [27]. It should be noted that a

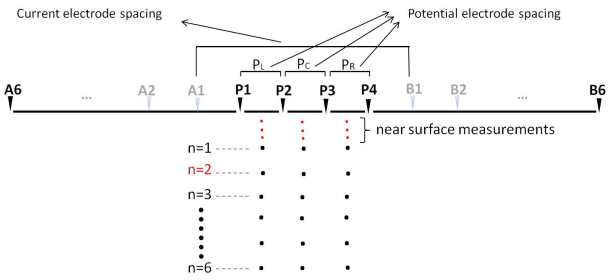

Figure 1: Schematic survey line of typical CRSP array

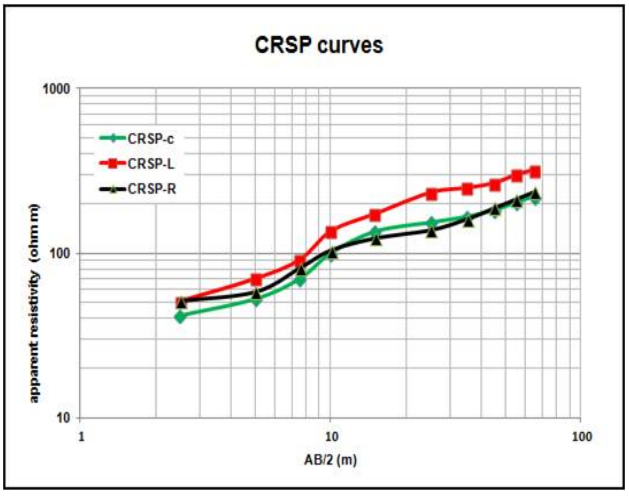

Figure 2: Typical sounding curves of CRSP (left (L), centre (C) and right (R)) array

combined method, called "Combined Sounding-Profiling Resistivity" was also proposed by [28]. This method is significantly different from CRSP in each of electrode configuration, field operation, and processing. For example, in the Karous and Pernu proposed array, the distance between potential electrodes is constant, but in the CRSP configuration, three couples of potential electrodes are used (PL, PC, and PR). Likewise, the Karous and Pernu configuration is based on a three-electrode array, while a symmetrical array is used in the CRSP method [26].

Figure 2 illustrates three CRSP sounding curves along a measurement station with the unit potential electrode spacing of 10 meters as well as measurement points' distance, minimum potential electrode spacing of 1 meter and maximum current electrode spacing of 130 meters.

3 CRSP performance

The sensitivity function given by the Frechet derivative [29] basically is about the degree to which a change in the re-

Table 1: Median depth of investigation of some different arrays for different values of "n" in comparison with CRSP measurements (shaded cells). CRSP-c and pole-dipole show same depth of investigation indexes. Note that pole dipole array needs a physical infinite current electrode and hence its position affects on survey results.

Array	n=1	n=2	n=3	n=4	n=5	n=6	n=7
CRSP-C	0.519	0.925	1.318	1.706	2.093	2.478	2.863
CRSP-L, R	-	0.579	1.053	1.495	1.918	2.329	2.733
Wenner	0.519	-	-	-	-	-	-
wenner-Schlumberger	0.519	0.925	1.318	1.706	2.093	2.478	2.863
Linear dipole-dipole	0.416	0.697	0.962	1.220	1.476	1.730	1.983
Linear pole-dipole	0.519	0.925	1.318	1.706	2.093	2.478	2.863
pole-pole	0.867	-	-	-	-	-	-

sistivity of a section of the subsurface will influence the potential measured by the array [7]. Hence the image produced by different arrays over the same structure can be very different because of differences in the sensitivity function of the arrays for a certain earth model.

As mentioned before, each electrode array has its own characteristics of advantages and disadvantages. (i) The depth of the targets, (ii) the respond to lateral and vertical variations and (iii) the amount of field coverage related to total profile length are three properties with which CRSP performance have been evaluated in this paper.

According to [30], potential difference ($\partial\varphi$) due to resistivity change ($\partial\rho$) in a very small volume of the ground located at (x, y, z) measured on the surface by a single current electrode located at (a,0,0) and a single potential electrode located at (b,0,0) is given by following formulation:

$$\frac{\partial\varphi}{\partial\rho} = \frac{1}{\rho^2}\int \nabla\varphi.\nabla\varphi' dv \tag{1}$$

Where:

$$\varphi = \frac{\rho}{2\pi\sqrt{((x-a)^2+y^2+z^2)}}$$

and

$$\varphi' = \frac{\rho}{2\pi\sqrt{((x-b)^2+y^2+z^2)}}$$

Potential φ is result of injecting 1 ampere to current electrode and potential φ' is the result of a current electrode located at potential electrode position. The inner term of the above integral is named as "sensitivity function" [29]. For 1D sounding, the depth of investigation could be estimated by integrating equation (1) in horizontal (x, y) directions:

$$sF_{1d}(z) = \int_{-\infty}^{\infty}\int \frac{1}{4\pi^2} \tag{2}$$

$$\cdot \frac{(x-b)(x-a)+y^2+z^2}{\sqrt[3]{(x-a)^2+y^2+z^2}\times\sqrt[3]{(x-b)^2+y^2+z^2}}dxdy$$

The solution of equation (2) is given by [31]:

$$sF_{1d}(z) = \frac{2}{\pi}\cdot\frac{z}{\sqrt[3]{(c)^2+4z^2)}} \tag{3}$$

Where

$$c = (b-a)$$

The above calculations should be done for 4 pairs of current-potential electrodes and to be added up to have 1D sensitivity function $sF_{1d}(z)$ for a general 4 electrode array. Figure 3 illustrates two plots of equation (3) for CRSP in n=3 and for centre, right and left measurements.

Equation (3) has been used by authors to mention the properties of various arrays in 1D resistivity measurements. According to [32] when the area under the curve reaches the half of the total area, the corresponding (ze/a) called as "median depth of investigation" could be a good estimation of depth of investigation.

Table (1) indicates CRSP median depth of investigation for different amounts of "n". This table also compares the median depth of investigation for some different arrays. The maximum Sensitivity value of each array is yielded in table (2) as it could be a good index of the vertical resolution of an array.

From Table (1) it can be concluded that the depth of investigation related to minimum electrode spacing of CRSP-C is more than dipole-dipole and it is equal to the Wenner-Schlumberger and Wenner. Note that although (z_e/a) values of median depth of investigation for CRSP are the same as pole–dipole too, their corresponding sensitivity values are almost 2 times higher than pole-dipole; it convincingly reveals more precise vertical resolution of CRSP array than pole-dipole array (table 2). Also CRSP yields a better lateral resolution due to more coverage of data in a survey line

Table 2: Maximum sensitivity values of some different arrays for different values of "n" in comparison with CRSP measurements.

Array	n=1	n=2	n=3	n=4	n=5	n=6	n=7
CRSP-C	0.2	0.0376	0.0132	0.0061	0.0033	0.0020	0.0013
CRSP-L, R		0.1032	0.0212	0.0081	0.004	0.0022	0.0014
Wenner	0.2	-	-	-	-	-	-
Wenner-Schlumberger	0.2	0.0376	0.0132	0.0061	0.0033	0.0020	0.0013
Linear dipole-dipole	0.0851	0.0128	0.0038	0.0027	0.0015	0.0007	0.0004
Linear pole-dipole	0.0994	0.0188	0.0066	0.0031	0.0017	0.001	0.0007
pole-pole	0.1213	-	-	-	-	-	-

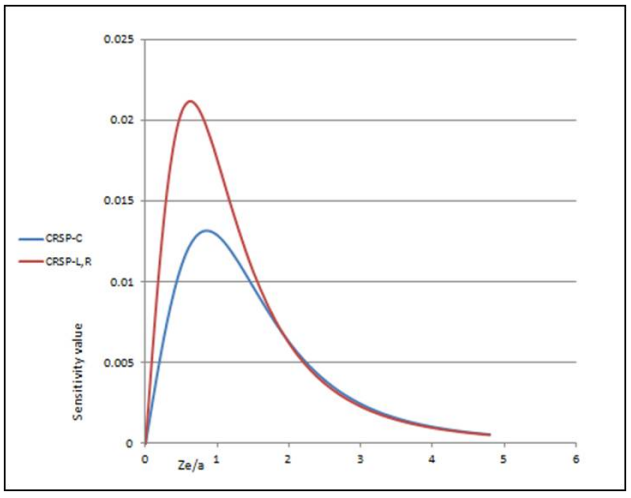

Figure 3: 1D sensitivity functions of CRSP measurements for n=3. The red curve shows sensitivity function of central measurements while the blue curve is related to left and right measurement.

(three measurements are acquired for each "n") in reasonable time consumption in comparison with the Wenner - Schlumberger array.

4 The synthetic model testing

In this section, synthetic cavities are modeled in different geological situations, and then the responses of different types of electrode configurations are compared with results arisen from CRSP array. Empty voids are assumed to be very high resistive bodies; so they are indicated as high resistivity anomalous zones in electrical resistivity inversion images [23]. Our intention is to detect the cavities, their geometry, and the depth of occurrences as well as the surrounding media geological properties. In all models forward modeling was carried out by the application of the RES2MOD freeware [33], and inversion by the application of the commercially available RES2DINV software. In the first case three rectangular bodies C1 with dimensions of 3×3 m and a depth of burial of 1.5 m, C2 with dimensions of 2×2 m and a depth of burial of 2 m, and C3with dimensions of 1.5×1.5 m and a depth of burial of 2.5 m are modeled as empty cavities with resistivity of 106 ohm-m embedded in a uniform media of 100 ohm-m (Figure 4-a). The e^m ployed electrode arrays are the Wenner, dipole-dipole, the Wenner-Schlumberger, and CRSP with 51 electrodes spread at 1 m intervals. Figures 44-b, 4-c, 4-d, and 4-e show the inversion resistivity section by dipole-dipole array, the Wenner, the Wenner-Schlumberger, and CRSP array, respectively. As seen in the figure, objectives in the results arisen from the Wenner array were detected as less intensive anomalies rather than the others. The anomalies in the figure 4-b have the most intensities while true dimensions and also depths of burial could be inferred from the image by CRSP array (figure 4-e).

The second model consists of two layers as shown in figure 5-a. The top layer has an electrical resistivity value of 50 ohm-m and a thickness of 33 meters. The second layer is a uniform half-space with an electrical resistivity value equal to 200 ohm-m. A cavity of 10^6 ohm-m and 21 m in diameter is inserted in a burial depth of 9 m. The employed electrode arrays are the Wenner, dipole-dipole, the Wenner-Schlumberger, and CRSP with 51 electrodes spread at 10 m intervals. Figures 5-b, 5-c, 5-d, and 5-e show the inversion resistivity section by dipole-dipole array, the Wenner, the Wenner-Schlumberger, and CRSP array, respectively. The cavity was detected in the inverted image from dipole-dipole array as a nearly vertical resistive anomaly with an average of approximately 15 meters in diameter, while it was nearly indistinguishable in the image from the Wenner array. Images from the Wenner-Schlumberger and CRSP array could detect the layers intersection very well, while the cavity in the figure 5-e is highlighted as a very high resistivity anomaly with an average diameter of nearly 20 meters. Depth of investigation in the figure 5-b is less than the others.

The third model describes a vertical normal fault accruing in a three strata sedimentary medium. The electri-

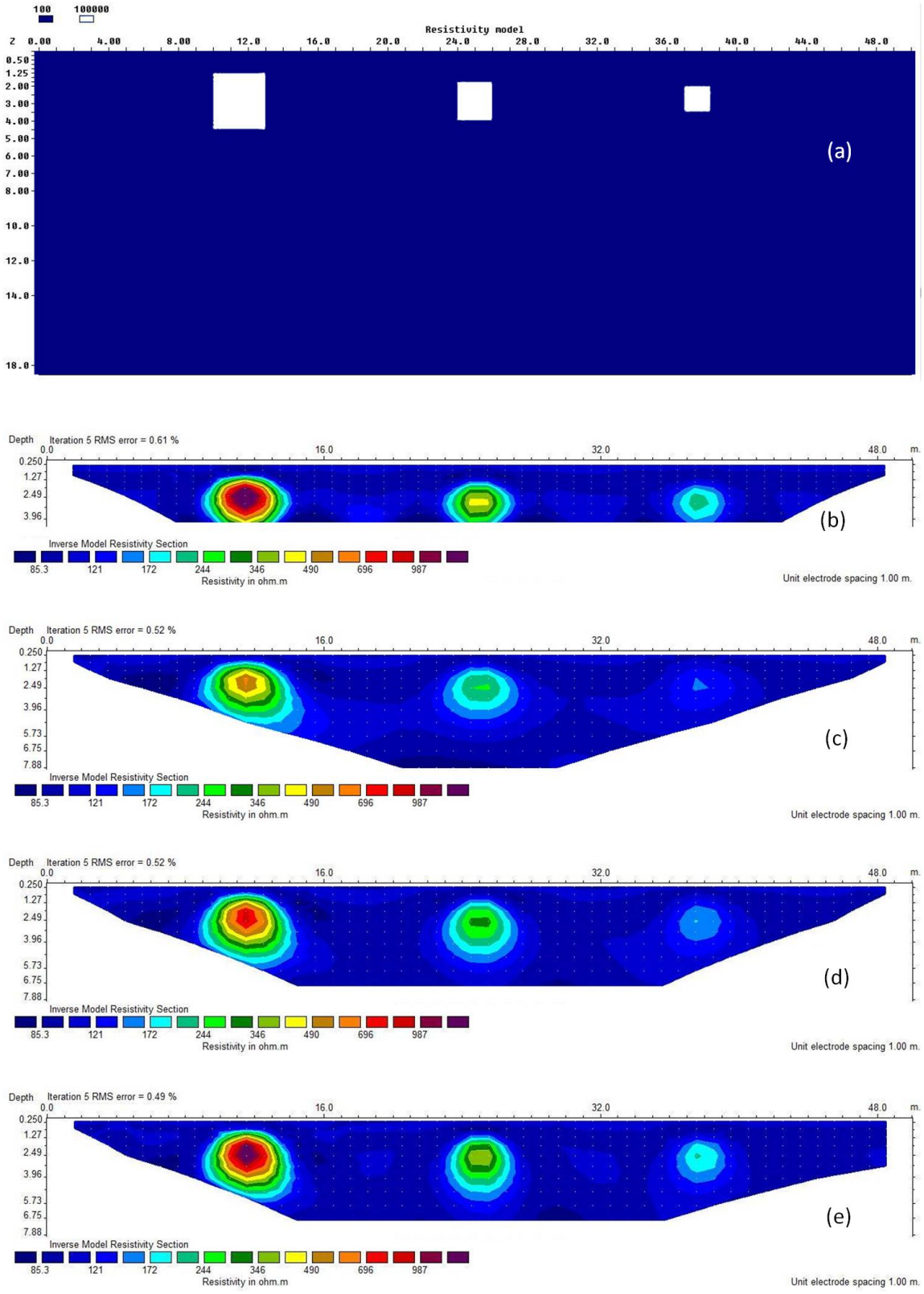

Figure 4: (a) model of cavities inserted in a uniform media, (b) the resistivity inversion image from dipole-dipole data, (c) the resistivity image from the Wenner data, (d) the resistivity image from the Wenner-Schlumberger data, and (e) the resistivity image from CRSP data.

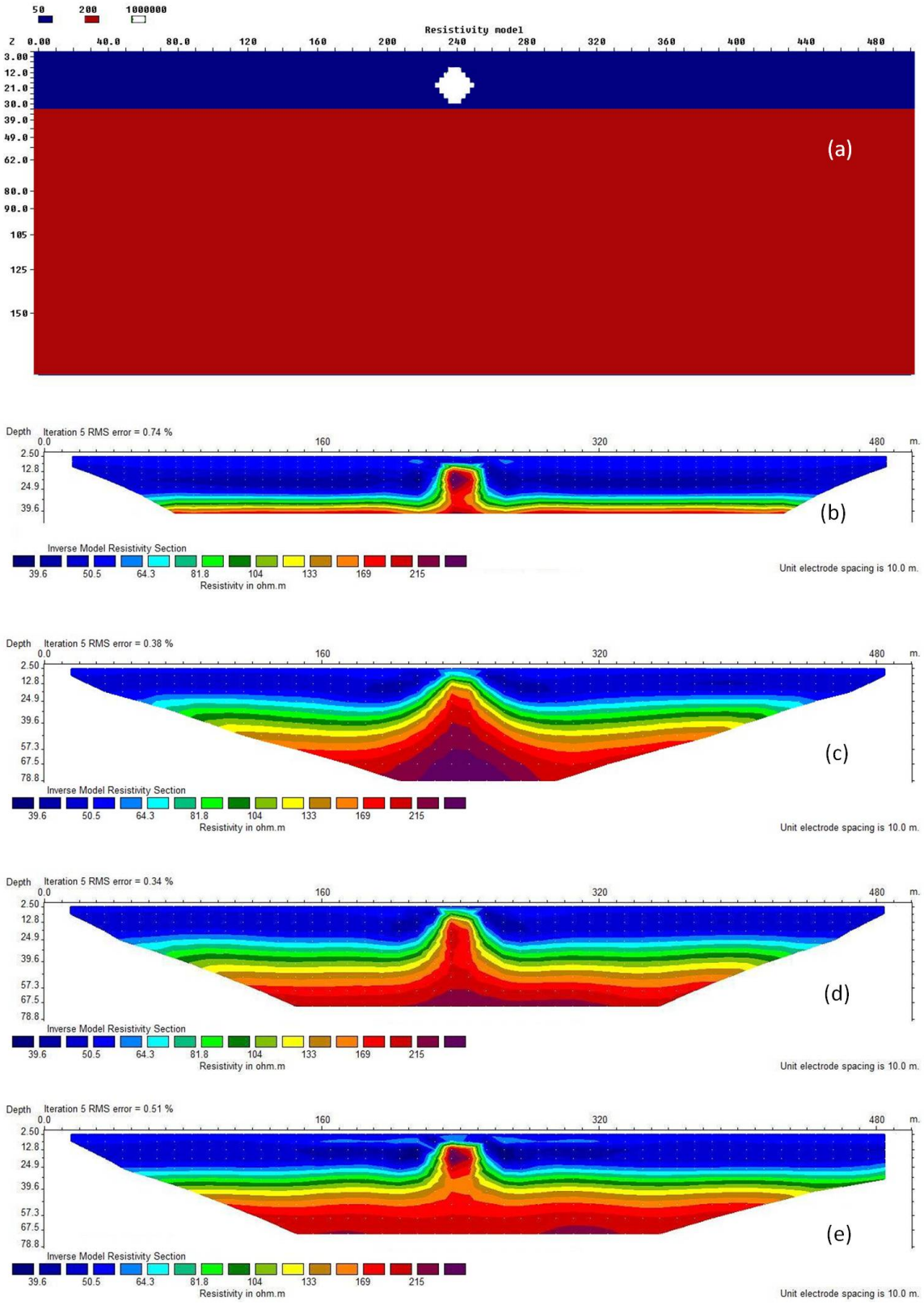

Figure 5: (a) model of a cavity inserted in a two layered media, (b) the resistivity inversion image from dipole-dipole data, (c) the resistivity image from the Wenner data, (d) the resistivity image from the Wenner-Schlumberger data, and (e) the resistivity image from CRSP data.

cal resistivity values of top layers are 100 and 400 ohm-m with thicknesses of 10 m and 35 m, respectively, overlying 50 ohm-m bedrock. The covering top layers are assumed to be leveled due to erosion. A rectangular body of empty void of 10^6 ohm-m with dimensions of 15×20 m and a burial depth of 15 m is inserted in the second layer, as illustrated in Figure 6-a. The employed electrode arrays are the Wenner, dipole-dipole, the Wenner-Schlumberger, and CRSP with 51 electrodes spread at 10 m intervals. 3 percent Gaussian noise was added to the responses from the arrays. Figures 6-b, 6-c, 6-d, and 6-e show the resulting inversion resistivity section by dipole-dipole array, the Wenner, the Wenner-Schlumberger, and CRSP array, respectively. From the figure it could be inferred that the least noise effect belongs to the inverted image from the Wenner array. Likewise the fault was detected in the figure 6-c with more precision rather than the others. Although the cavity was detected in all the images, its dimensions was exaggerated in figure 6-b (about 40×20 m). Finally as seen in figure 6-e the inverted image from CRSP array shows a more reliable picture of the model than other array types as the dimensions of the detected cavity are estimated to be about 20×15 m and resistivity of the second layer wherein the cavity is surrounded, was detected as a resistivity layer of 450-500 ohm-m.

5 Field case study: Abshenasan expressway U-turn bridge site investigation, Tehran, Iran

Civil engineering projects are always dealt with geological problems and geotechnical issues. Conducting these projects in urban areas has several critical and special problems. Lack of scientific attention to them can cause noticeable damages or even disasters. Channels, underground cavities, wells, aqueducts and other obsolete manmade underground structures which may be buried now or in the near future, are among the most crucial geotechnical and geological problems in urban areas. In Iran, systems of underground aqueducts called Qanats were constructed in past millenniums, a series of well-like vertical shafts with depths from 1 m to more than 80 m, connected by gently sloping tunnels [34]. This technique taps into subterranean water in a manner that delivers water to the surface without the need for pumping. These kinds of underground void spaces (empty or filled with loose materials) usually cause weak points in the ground, they are in an urgent need to identify, map and compile. In this case study, the electrical resistivity approach was conducted to investigate Abshenasan expressway U-turn bridge site for detecting potentially existing cavities and/or loose materials. Abshenasan expressway is one of important expressways in north of the capital city of Tehran, Iran (Figure 7-a). Tehran is characterized with the existence of vast amounts of Qanats. The depth of the Qanat shafts in Tehran ranges from 3 m to more than 35 m; likewise Qanat tunnels are usually 1m to 2 m in diameter and their length varies depending on the distance of contiguous shafts. Although the number of the Qanats in Tehran is claimed to be more than 500, the real number of them is estimated to be more than 2000. Most of the Qanats are obsolete nowadays [35].

As mentioned before, electrode configuration is one of the most important factors to design a precise and appropriate survey. An unsuitable designation can lead to poor quality of obtaining data and wrong results in some cases. According to geological and geotechnical investigations, the area is covered by Quaternary fine grain alluviums with a thickness of more than 10 m. most of the study region is leveled during urban facilities constructing. Also a Qanat shaft is seen in the study area suggesting a passing Qanat system. With regard to the mentioned properties of the study area and geometric and electrical properties of probable channels and/or loose materials, electrical resistivity profiling approach was carried out by CRSP array.

For each pier foundation Electrical surveying was performed with respect to below criteria:

- Full coverage of data points along with the profiles
- Adequate accuracy of data to detect anomalies
- Resistivity could be obtained by interpretation of sounding curves.

Hence, in this case study, CRSP resistivity measurements were acquired along eight survey lines. Figure 7-b shows the locations of designated survey lines. In all survey lines the measuring point interval as well as potential electrode spacing was assigned to 5 m. For AB shorter than 25 m, the distance of each couple of the potential electrodes was decreased to 2 m, and each one of the sounding points was separately surveyed (n=1). Survey lines P1 to P3 consist of seven stations each 35 m in length. 70 measurements were acquired along each profile covering southern piers of Abshenasan U-turn Bridge.

Survey line P4 was 30 meters in length and consists of two stations. 70 measurements were recorded along this survey line covering the central pier foundation of Abshenasan U-turn Bridge.

Survey lines P5 to P8 consist of four stations. 70 measurements were recorded along the survey lines P5 to P8 to cover northern piers' foundations of the U-turn Bridge.

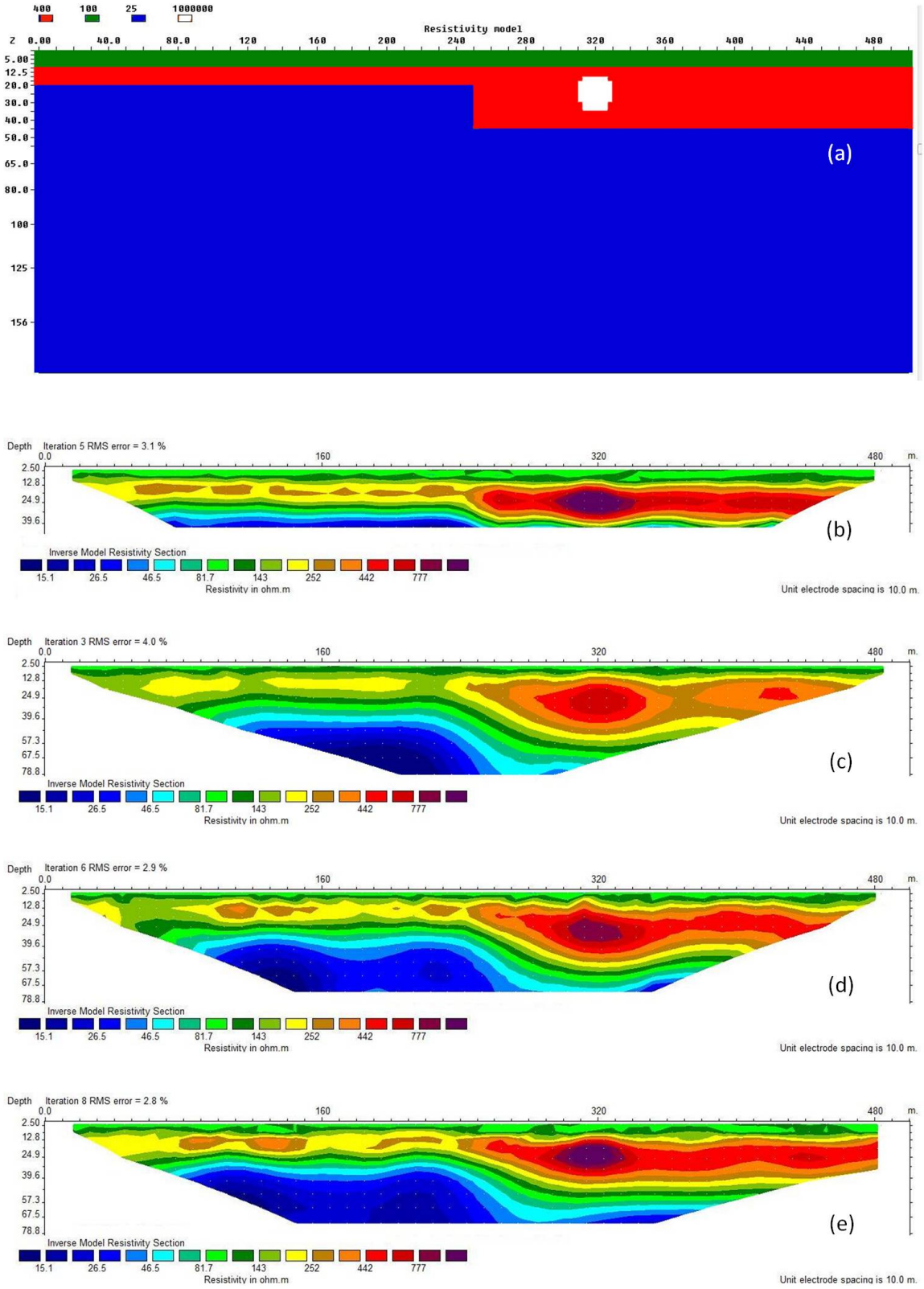

Figure 6: (a) model of a cavity inserted in a three layered media with a normal vertical fault, (b) the resistivity inversion image from dipole-dipole data, (c) the resistivity image from the Wenner data, (d) the resistivity image from the Wenner-Schlumberger data, and (e) the resistivity image from CRSP data.

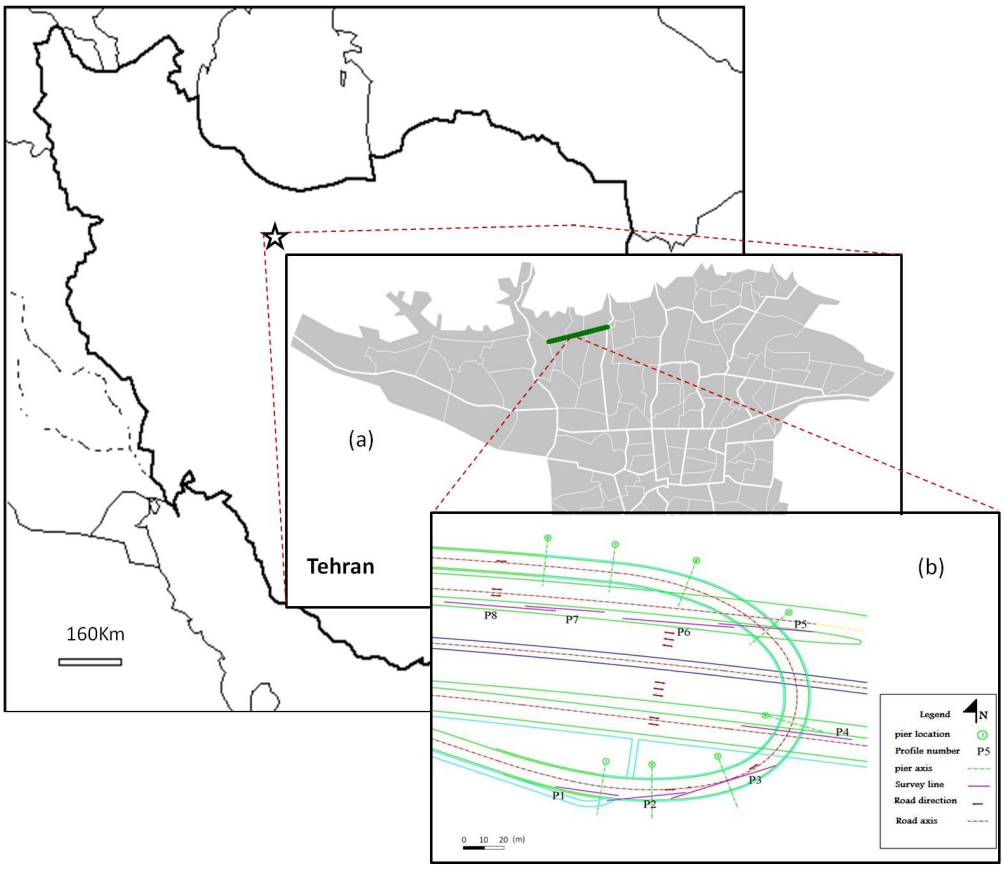

Figure 7: (a) location of Abshenasan expressway in Tehran, Iran and (b) location of designed survey lines in Abshenasan Expressway U-turn Bridge.

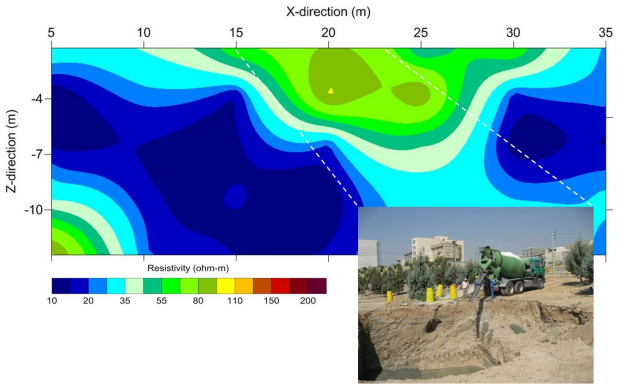

Figure 8: Electrical resistivity inverted image along survey line P1.

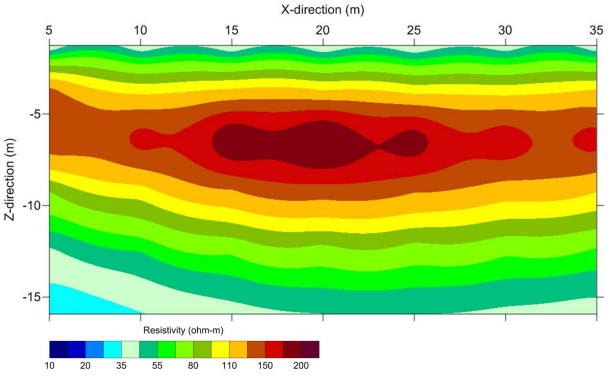

Figure 9: Electrical resistivity inverted image along survey line P4.

Results of survey lines P1, P4 and P7 are presented in Figures 8 to 10 in the form of 2D resistivity inversion images. The resistivity inversion image along the profile P1 is illustrated in the figure8. As is shown in the figure, the results show no important anomalous phenomena. Resistivity is in background range throughout the section. A smooth increscent of resistivity in the central part of the section and in depths of 0 to 7 meters is seen. A Qanat shaft exists in 3 meters north of survey line P1seems to be responsible for the anomaly (point A in Figure 8)

The resistivity inversion image along profile P4 is illustrated in Figure 9. As shown, there is a high resistivity anomaly in the figure. This anomaly is interpreted as a horizontal pipe in depth of 4.5 to 6 m.

Figure 10: the Qanat tunnel detected in inverted image along survey line P4.

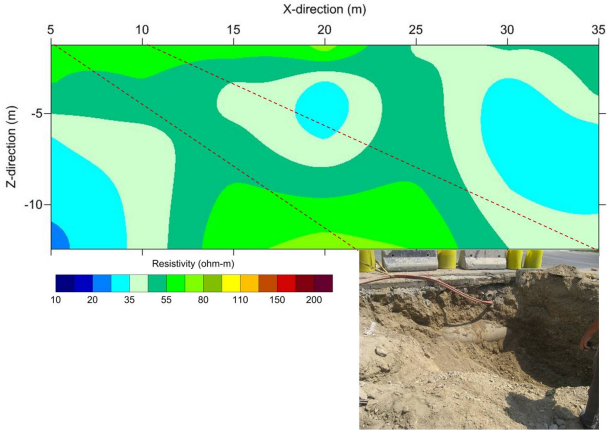

Figure 11: Electrical resistivity inverted image along survey line P7 at Abshenasan U-turn bridge site.

We guessed this anomaly could be a horizontal cavity like a tunnel. Therefore, we suggested excavating a trench perpendicular to the survey line P4. Observations showed that an aqueduct tunnel exists in depth about 5 m (Figure 10). It is nearly parallel to the profile and about 2 meters (horizontally) north of it. The average diameter of the tunnel is nearly 1.3 meters.

Figure 11 belongs to the resistivity inversion image along survey line P7. The image shows a relatively high resistivity anomaly at western part of the section. The anomaly seems to be the result of a backfilled hole; hence excavation was suggested in the area. Observations showed an area containing loose coarse grained materials.

6 Conclusion

In this paper, Combined Resistivity Sounding and Profiling array was introduced to detect underground cavities with an acceptable precision in different situations. A comparison between conventional arrays and CRSP in terms of 1D sensitivity values and median depths of investigation reveals convincingly that the depth of investigation of CRSP-C is more than dipole-dipole and is equal to the Wenner-Schlumberger and pole-dipole. It should be noted that the sensitivity value of CRSP-C for each “n” is almost two times as high as pole-dipole, which suggests more precision of CRSP in vertical resolution. Also in comparison with the Wenner - Schlumberger array, CRSP yields a better lateral resolution due to more coverage of data in a survey line (three measurements are acquired for each "n"). Also the comparison between conventional arrays and CRSP in terms of synthetic model testing showed the reliability of the CRSP array in detection of the cavities in different situations; however, empirical tests are needed to confirm the results. Finally, in a field case study CRSP array was applied to conduct electrical resistivity method in Abshenasan expressway U-turn Bridge site for detecting potential cavities and/or filling loose materials. The results led to detect an aqueduct tunnel passing beneath the study area. The results were confirmed by surface excavations.

References

[1] G. K. Anudu, B. I. Essien and S. E. Obrike, "Hydrogeophysical investigation and estimation of groundwater potentials of the Lower Paleozoic to Precambrian crystalline basement rocks in Keffi area, north-central Nigeria, using resistivity methods," *Arabian Journal of Geosciences*, vol. 7, no. 1, pp. 311-322, 2014.

[2] S. Yilmaz and C. Narman, "2-D electrical resistivity imaging for investigating an active landslide along a ridgeway in Burdur region, southern Turkey," *Arabian Journal of Geosciences*, 2014.

[3] M. Bayrak and L. Senel, "Two-dimensional resistivity imaging in the Kestelek boron area by VLF and DC resistivity methods," *Arabian Journal of Geosciences*, vol. 82, pp. 1-10, 2012.

[4] C. Fehdi, F. Baali and D. Boubaya, "Detection of sinkholes using 2D electrical resistivity imaging in the Cheria Basin (north–east of Algeria)," *Arabian Journal of Geosciences*, vol. 4, no. 1, pp. 181-187, 2011.

[5] M. E. Candansayar and A. T. Basokur, "Detecting small-scale targets by the 2D inversion of two-sided three-electrode data: application to an archaeological survey," *Geophys Prospect*, vol. 49, no. 1, pp. 13-25, 2001.

[6] E. A. Atekwana, W. A. Sauck and D. D. Werkema, "Investigations of geoelectrical signatures at a hydrocarbon contaminated site," *J. Appl. Geophys*, vol. 44, pp. 167-180, 2000.

[7] M. H. Loke, "Tutorial: 2-D and 3-D electrical imaging surveys, Course Notes for USGS Workshop: 2-D and 3-D Inversion and Modeling of Surface and Borehole Resistivity Data," 2001.

[8] M. H. Loke and R. D. Barker, "Rapid least-squares inversion of apparent resistivity pseudosections by a quasi-Newton method," *Geophysical Prospecting*, vol. 44, pp. 131-152, 1996.

[9] S. Narayan, M. B. Dusseault and D. C. Nobes, "Inversion techniques applied to resistivity inverse problems," *Inverse Problems*, vol. 10, no. 3, 1994.

[10] N. G. Papadopoulos, G. N. Tsokas, M. Dabas, M. G. Yi and P. Tsourlos, "3D Inversion of Automated Resistivity Profiling (ARP) Data," *ArcheoScience*, vol. 33, pp. 329-332, 2009.

[11] M. M. Nordiana, S. Rosli and M. N. M. & Nawawi, "A numerical comparison of enhancing horizontal resolution (EHR) technique utilizing 2D resistivity imaging," *Arab J. Geosciences*, vol. 7, no. 1, pp. 299-309, 2014.

[12] T. Henning, A. Weller and T. Canh, "The effect of dike geometry on different resistivity configurations," *Applied Geophysics*, vol. 57, no. 4, p. 278–292, 2005.

[13] T. Dahlin and B. Zhou, "A numerical comparison of 2D resistivity imaging with 10 electrode arrays," *Geophysical Prospecting*, vol. 52, no. 5, p. 379–398, 2004.

[14] A. Dey and H. F. Morrison, "Resistivity modeling for arbitrariy shaped two dimensional structures," *Geophysical Prospecting*, vol. 27, pp. 106-136, 1976.

[15] L. Orlando, "GPR to constrain ERT data inversion in cavity searching: theoretical and practical applications in archeology," *J. Appl. Geophys*, vol. 89, pp. 35-47, 2013.

[16] P. Thierry, N. Debeblia and A. Bitri, "Geophysical and geological characterisation of karst hazards in urban environments: application to Orléans (France)," *Bulletin of Engineering Geology and the Environment*, vol. 64, no. 2, pp. 139-150, 2004.

[17] F. Gizzi and N. Masini, "Historical damage pattern and differential seismic effects in a town with ground cavities: a case study from Southern Italy," *Engineering Geology*, vol. 88, no. 1-2, pp. 41-58, 2006.

[18] A. Amini and H. Ramazi, "Application of electrical resistivity imaging for engineering site investigation. A case study on a prospective hospital site, Varamin, Iran," *Acta Geophysica*, p. accepted manuscript, 2016.

[19] K. Chalikakis, V. Plagnes, R. Guerin, R. Valois and F. P. Bosch, "Contribution of geophysical methods to karst-system exploration: an overview," *Hydrogeology Journal*, vol. 19, pp. 1169-1180, 2011.

[20] M. Abu-Shariah, "Determination of cave geometry by using a geoelectrical resistivity inverse model," *Engineering Geology*, vol. 105, no. 3, pp. 239-244, 2009.

[21] A. P. Aizebeokhai, A. I. Olayinka and V. S. Singh, "Application of 2D and 3D geoelectrical resistivity imaging for engineering site investigation in a crystalline basement terrain, southern Nigeria," *Environmental Earth Sciences*, vol. 61, pp. 1481-1492, 2010.

[22] W. Zhou, B. F. Beck and A. L. Adams, "Effective electrode array in mapping karst hazards in electrical resistivity tomography," *Environmental Geology*, vol. 42, p. 922–928, 2002.

[23] M. Van Schoor, "Detection of sinkholes using 2D electrical resistivity imaging," *Applied Geophysics*, vol. 50, p. 393–399, 2002.

[24] H. R. Ramazi, "Combined resistivity sounding and profiling and its application in mineral exploration and site investigation," Tehran (in persian), 2005.

[25] A. Amini and H. Ramazi, "Anomaly enhancement in 2D electrical resistivity imaging method using a residual resistivity technique," *The Journal of The Southern African Institute of Mining and Metallurgy*, vol. 116, pp. accepted manuscript, under publication, 2016.

[26] H. Ramazi and M. Jalali, "Contribution of geophysical inversion theory and geostatistical simulation to determine geoelectrical anomalies," *Stud. Geophys. Geod*, 2014.

[27] H. Ramazi and K. Mostafaie, "Application of integrated geoelectrical methods in Marand (Iran) manganese deposit exploration," *Arab J. Geosciences*, vol. 6, no. 8, pp. 2961-2970, 2013.

[28] M. Karous and T. K. Pernu, "Combined sounding profiling resistivity measurements with the three electrode arrays," *Geophys Prospect*, vol. 33, pp. 447-459, 1985.

[29] P. R. McGillivray and D. W. Oldenburg, "Methods for calculating Frechet derivatives and sensitivities for the non-linear inverse problem: A comparative study," *Geophysical Prospecting*, vol. 38, pp. 499-524, 1990.

[30] M. H. Loke and R. D. Barker, "Least-squares deconvolution of apparent resistivity pseudosections," *Geophysics*, vol. 60, pp. 1682-1690, 1995.

[31] A. Roy and A. Apparao, "Depth of investigation in direct current methods.," *Geophysics*, vol. 36, pp. 943-959, 1971.

[32] L. S. Edwards, "A modified pseudosection for resistivity and induced-polarization," *Geophysics*, vol. 42, pp. 1020-1036, 1977.

[33] M. H. Loke, *RES2DMOD, 2D resistivity and IP forward modeling, Ver. 3.0, Freeware, www.geotomosoft.com/r2dmodwin.zip [accessed 12 Jun 2014]*, 1995-2013.

[34] A. Semsar Yazdi and S. Askarzadeh, "A historical review on the Qanats and historichydraulic structures of Iran since the first millennium B.C.," in *International History Seminar on Irrigation and Drainage*, Tehran, Iran, 2007.

[35] I. Tehran Municipality. [Online]. Available: http://tdmmo.tehran.ir/Default.aspx?tabid=190. [Accessed 1 Sep 2015].